ASIA-PACIFIC METROLOGY PROGRAMME
100 MPa GAS PRESSURE INTERLABORATORY COMPARISON
Comparison Identifier: **APMP.M.P-S6**

Final Report on Supplementary Comparison APMP.M.P-S6 in Gas Gauge Pressure from 10 MPa to 100 MPa

October 2015

Hiroaki Kajikawa[1], Douglas A. Olson[2], Hideaki Iizumi[1], Robert Greg Driver[2], Momoko Kojima[1]

[1]NMIJ/AIST (Pilot institute): National Metrology Institute of Japan, AIST, AIST Tsukuba Central 3, 1-1, Umezono 1-Chome, Tsukuba, Ibaraki, 305-8563 Japan

[2]NIST: National Institute of Standards and Technology, 100 Bureau Drive, MS 8364 Gaithersburg, MD 20899-8364, USA

Abstract

A supplementary comparison of gas high-pressure standards was conducted between the National Metrology Institute of Japan (NMIJ/AIST) and the National Institute of Standards and Technology (NIST), within the framework of the Asia-Pacific Metrology Programme (APMP), in order to determine their degrees of equivalence in the pressure range from 10 MPa to 100 MPa in gauge mode. The pilot institute was NMIJ/AIST. The measurements were carried out from July 2014 to October 2014. Both participating institutes used pressure balances as their pressure standards. Different gases were used for the pressure medium: NMIJ/AIST used Nitrogen, while NIST used Helium. A set of two pressure monitors was used as the transfer standard. The pressure monitors were found sufficiently stable during the measurements. Characteristics of the pressure monitors were evaluated at the pilot institute, and then used for data corrections and uncertainty estimations. In particular, the effect of the gas medium on the pressure monitors was found to be significant, and then all the measurement data were corrected to those with Nitrogen. The degrees of equivalence between the two institutes were evaluated by the relative differences of the participant's results and their associated expanded (k = 2) uncertainties. The gas pressure standards in the range 10 MPa to 100 MPa for gauge mode of the two participating institutes were found to be equivalent within their claimed uncertainties.

Contents

1. Introduction

The National Metrology Institute of Japan (NMIJ/AIST), Japan, has been approved by the Technical Committee for Mass and Related Quantities (TCM) in the Asia-Pacific Metrology Programme (APMP) to coordinate an interlaboratory comparison program in pressure as a pilot institute. The comparison was identified as **APMP.M.P-S6** by the Consultative Committee for Mass and Related Quantities (CCM) of the International Committee for Weights and Measures (CIPM), and APMP. The objective of the comparison is to compare the performance of gas pressure standards in the National Metrology Institutes (NMIs), in the pressure range 10 MPa to 100 MPa for gauge mode according to the guidelines [1,2,3]. The results of this comparison will be included in the Key Comparison Database (KCDB) of BIPM following the rules of the CCM and will be used to establish the degree of equivalence of national measurement standard by NMIs [4]. Degrees of equivalence are essential supporting evidence for calibration and measurement capabilities (CMCs) of NMIs as specified in the Mutual Recognition Arrangement (MRA) [1].

The comparison is a bilateral supplementary comparison between NMIJ/AIST, the pilot institute, and National Institute of Standards and Technology (NIST). A protocol was prepared by the pilot institute, and approved in July 2014 with some modifications. Two pressure monitors were used as the transfer standard. After the characterizations of the transfer standard, the measurements were conducted from July 2014 to October 2014, in the order of NMIJ/AIST, NIST, and NMIJ/AIST. The participants reported the readings of the pressure monitors and the pressure values of their standards with the associated uncertainties. The pilot institute analyzed the reported data and prepared a report of the comparison according to established guidelines[1,2,3,4].

The following sections provide descriptions of the participant's pressure standards, the transfer standard, the circulation of the transfer standard, the general measurement procedure, the method for analysis of the measurement data, the comparison of the results with the associated uncertainties, and the degree of equivalence between the participants.

2. Laboratory standards

2.1 List of participating institutes

Two National Metrology Institutes (NMIs) participated in this comparison including the pilot institute. The participating institutes along with their addresses are listed in Table 2.1.

Table 2.1: List of the participating institutes.

ID	Participating Institutes	Contact Persons
1	**Country:** Japan **Acronym:** NMIJ/AIST (Pilot institute) **Institute:** The National Metrology Institute of Japan, National Institute of Advanced Industrial Science and Technology **Address:** AIST Tsukuba Central 3, 1-1, Umezono 1-Chome, Tsukuba, Ibaraki, 305-8563 Japan	**Name:** Hiroaki Kajikawa Hideaki Iizumi Momoko Kojima **Tel:** +81-29-861-4378 **Fax:** +81-29-861-4379 **E-mail:** kajikawa.hiroaki@aist.go.jp h.iizumi@aist.go.jp m.kojima@aist.go.jp
2	**Country:** The United States of America **Acronym:** NIST **Institute:** National Institute of Standards and Technology **Address:** 100 Bureau Drive, MS 8364 Gaithersburg, MD 20899-8364	**Name:** Douglas A. Olson Robert Greg Driver **Tel:** 301-975-2956 **Fax:** 301-975-5969 **E-mail:** douglas.olson@nist.gov robert.driver@nist.gov

2.2 Pressure standards of participating institutes

Both the participating institutes used pressure balances of different manufacture[1] and model as their laboratory standards. Information about their standard

[1] Certain commercial equipment, instruments, materials, or software are identified in this paper to foster understanding. Such identification does not imply endorsement by NIST, nor does it imply that the items or software are necessarily the best available for the purpose.

that was used in this comparison is listed in Table 2.2. Details of their standards and traceability are explained in the following subsections.

Table 2.2: Summary of laboratory standards of the participating institutes.

		NMIJ/AIST	NIST
Pressure balance			
	Pressure balance base (Manufacturer, Model)	Fluke Calibration, PG7202-M	Ruska, 2475
	Weights	Nagano Keiki S/N HPD	Ruska S/N 40004
	Total mass of weights [kg]	100	68
	Relative uncertainty of mass [10^{-6}]	2.5	2.0
	Piston-cylinder unit	Fluke Calibration PC-7202-1 S/N: 874	Ruska Model: 2475-701 S/N: F-22
	Operation mode	Re-entrant, Liquid-lubricated	Re-entrant
	Pressure range [MPa]	1 to 100	9 to 104
	Material of piston	Tungsten carbide, Titanium	Tungsten carbide
	Linear thermal expansion coefficient [°C^{-1}]	4.50 x10^{-6}	4.55 x10^{-6}
	Material of cylinder	Tungsten carbide	Tungsten carbide
	Linear thermal expansion coefficient [°C^{-1}]	4.50 x10^{-6}	4.55 x10^{-6}
Effective area of piston-cylinder unit: $A_{p,tr} = A_{0,tr}$ (1 +λ_1 p + λ_2 p^2)			
	Reference temperature t_r [°C]	23	23
	$A_{0,tr}$ [mm^2]	9.803436	8.378298
	$u(A_{0,tr})$ / $A_{0,tr}$ [10^{-6}]	20.0	19.5
	λ_1 [MPa^{-1}]	-2.31x10^{-6}	-2.12x10^{-6}
	$u(\lambda_1)$ [MPa^{-1}]	Included in $u(A_{0,tr})$	Included in $u(A_{0,tr})$
	λ_2 [MPa^{-2}]	N/A	6.39x10^{-9}
	$u(\lambda_2)$ [MPa^{-2}]	N/A	Included in $u(A_{0,tr})$

2.2.1 NMIJ/AIST

The NMIJ/AIST gas pressure standard for pressures above 7 MPa is established using a pressure balance equipped with a liquid-lubricated piston-cylinder, manufactured by Fluke calibration, model PG7202-M. The effective area of the piston-cylinder used in this comparison was determined by cross-float measurements with a hydraulic free-deformation (FD) piston-cylinder (1 MPa/kg). The hydraulic FD piston-cylinder was used for the hydraulic pressure comparison CCM.P-K7 [5], and is traceable through a series of calibrations to larger piston-cylinder assemblies whose effective areas have been evaluated by the NMIJ/AIST mercury manometer and dimensional measurements. The effective area of the liquid-lubricated piston-cylinder over the whole pressure range is expressed by a linear function of pressure: $A = A_0 * (1 + \lambda_1 * p)$.

2.2.2 NIST

The NIST working standard used in this comparison is designated as PG87. It is a Ruska 2475-701 high pressure gas piston gauge which uses helium as the working fluid. Its calibration coefficients and their uncertainty (A_0, λ_1, and λ_2) were determined by a crossfloat against NIST hydraulic piston gauge PG41 using an oil-gas interface. PG41 receives its traceability through two NIST controlled clearance primary standard piston gauges. The traceability of PG87 through PG41 to the primary standards, along with its uncertainty, is documented in ref. [6].

The masses used on PG87 were calibrated by the NIST Mass Group. They are traceable to NIST mass standards, which are traceable to the IPK at the BIPM.

3. Transfer standard

Pressure monitors

Two pressure monitors are used as the transfer standard to provide redundancy and ensure reliability. Specifications of the pressure monitors are listed in Table 3.1.

Table 3.1: Pressure monitors used as the transfer standard

	Pressure monitor A	Pressure monitor B
Manufacturer	Fluke calibration	Paroscientific, Inc.
Model	RPM4 A100Ms	745-15K
Serial number	2081	126312
Sensor	Quartz reference pressure transducer (Q-RPT)	Digiquartz® Transducer

Pressure range	100 MPa	103 MPa (15,000 psi)
Resolution	0.0001 %	0.00001 %
Normal operating temperature range	15 ^{o}C to 35 ^{o}C	0 ^{o}C to 40 ^{o}C
Power supply	85 to 264 VAC, 50/60 Hz,	110V or 220V AC
Weight	5 kg	1.8 kg

Structure of transfer standard

The schematic of the transfer standard is shown in figure 3.1. The sizes of the transfer standard are approximately 630 mm (W) x 400 mm (D) x 270 mm (H), and the total weight is about 25 kg. The two pressure monitors are placed on an aluminum base plate. They are connected with each other by using high pressure tubes and fittings. A Bourdon tube pressure monitor is used to monitor pressure in the pressure tube. A thermocouple is used to measure the temperature in the pressure tube during measurements. A bubble level is used to adjust the level of the base-plate. The top of the reference bar indicates the reference level of the two pressure monitors: the height of the center of the pressure inlets. The height difference between the top of the bar and the top surface of the base plate is 74 mm. An environmental measuring device (TR-73U) is placed on the base plate to check the environmental conditions (temperature, relative humidity, and atmospheric pressure) during the comparison including the transportation.

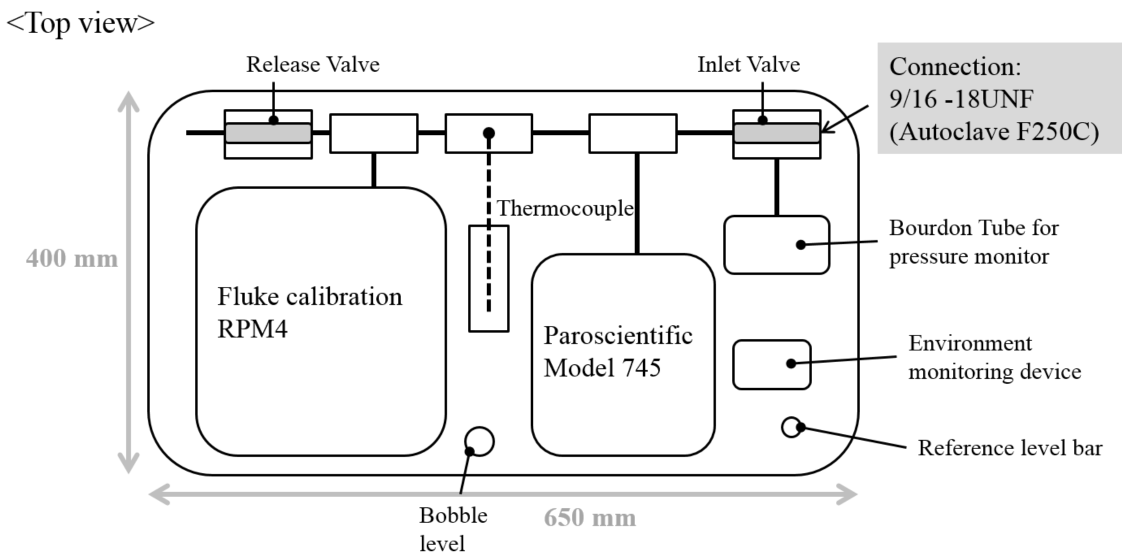

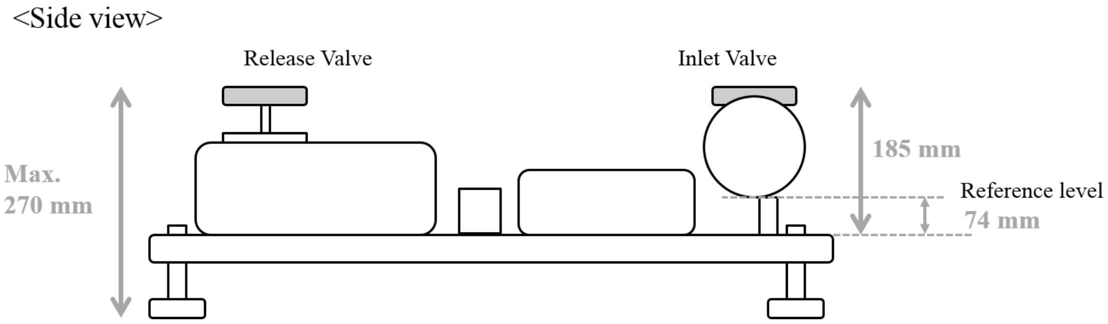

Figure 3.1: Schematic drawing of the transfer standard

Transfer package

The transfer standard and other accessories, listed in Table 3.2, are placed in a special carrying box. The dimensions of the box are approximately 840 mm (W) x 570 mm (D) x 380 mm (H), and the total weight is about 38 kg. Gravity shock recorders are placed on the bottom of the box to monitor the transporting conditions during the circulation. The estimated value of all the components was about 4,660,000 JPY. Photographs of the transfer standard and transfer package are shown in Figure 3.2.

Table 3.2: Contents of the transfer package

Item	Description	Number
Carrying box	SHOK-STOP SH	1
Transfer standard	- Pressure Monitor (RPM4 A100Ms) - Pressure Monitor (745-15K) - Bourdon tube pressure gauge - Environmental measuring device (TR-73U) Above devices are mounted on Al base plate.	1
Power cable	For both pressure monitors (identified by labels)	2
Temperature data logger	For thermocouple, Model TR-55i	1
Gravity shock recorder	G-MEN DR20 [Accelerations along three axes] with external battery	1
Operation and maintenance Manual	For pressure monitors (Fluke Calibration RPM4 [7], Paroscientific Model 745[8])	2
Protocol	Document	1

Figure 3.2: Transfer standard and transfer package for APMP.M.P-S6.

4. Circulation of transfer standard

4.1 Chronology of measurements

According to the protocol [9], the transfer package was circulated during the period from July 2014 to October 2014 in the order of NMIJ/AIST, NIST and NMIJ/AIST. The time period for measurement at each institute was four weeks after the arrival of the transfer standard. Time interval for transportation from one institute to the other was set to be within two weeks. The ATA carnet was attached to the transfer package, and used to avoid custom duties. The departure and arrival dates, and the condition of the transfer standard were reported to the other institute using the templates of Arrival report (appendix A1 in the protocol) and Departure report (appendix A2). The actual arrival and departure dates of the transfer standard, and the measurement dates for the three cycles are listed in Table 4.1. The transportation from NIST to NMIJ/AIST was delayed due to the custom procedures, but the delay did not affect the overall schedule.

Table 4.1: Chronology of measurements.

Institute	Arrival	Measurements	Departure
NMIJ/AIST	---	Jul. 30, 31, Aug. 1	Aug. 7
NIST	Aug. 21	Aug.29, Sep. 11, 12	Sep. 19
NMIJ/AIST	Oct. 9	Oct. 15, 17, 21	---

4.2 Environmental conditions during transportations

A gravity shock recorder and an environment monitoring device were used to check the conditions during transportations. The environment monitoring device measured temperature, atmospheric pressure, and relative humidity. The gravity shock recorder measured accelerations along three axes. The measured data were automatically recorded on the internal memory, and extracted from the memory at the pilot institute after the circulation.

Environmental conditions during transportations from NMIJ/NIST to NIST and vice versa were shown in Figure 4.1 and Figure 4.2, respectively. In each figure, figure (a) shows the acceleration; the data for three axes are combined to produce the absolute value of a total impact. From the acceleration data, we can see when the transfer standard is moved and when an impact is applied to the transfer standard. Impacts were applied mainly at airports before and after the air-freight. Figure (b) shows the temperature. The transfer standard was kept at moderate temperatures during the transportations. From the atmospheric pressure in figure (c), we can see when the transfer standard is carried by air-freight. The humidity, shown in figure (d), ranged from 40 % to 60 %. From the data, the transfer standard was carried in a careful manner, and kept under appropriate environmental conditions on the whole. In addition, no severe damages nor defects were reported from the participants.

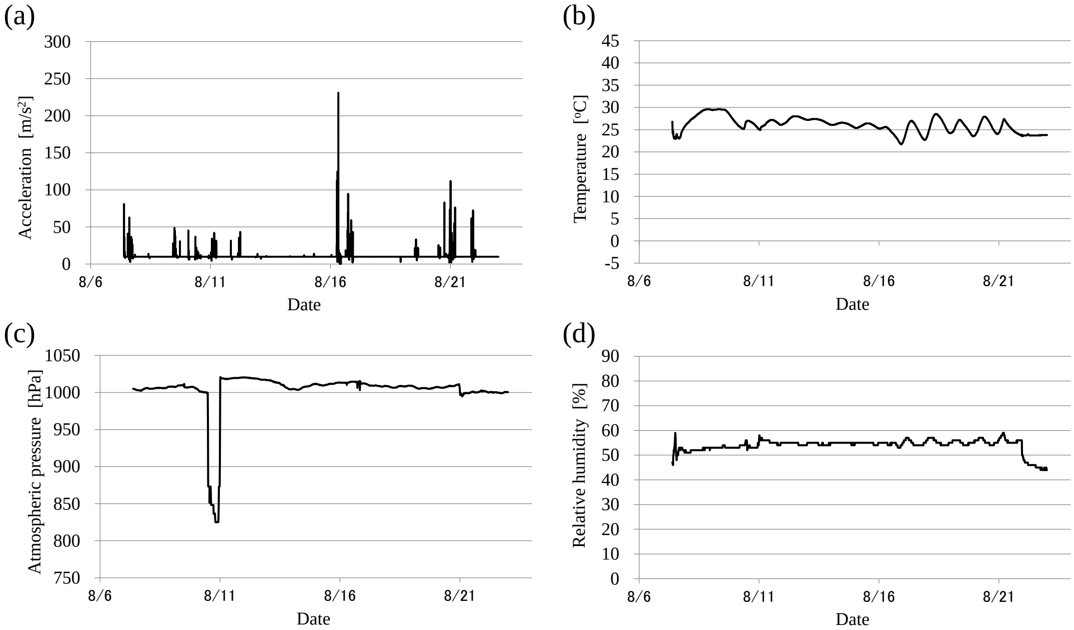

Figure 4.1: Environmental conditions during transportation from NMIJ/AIST to NIST.

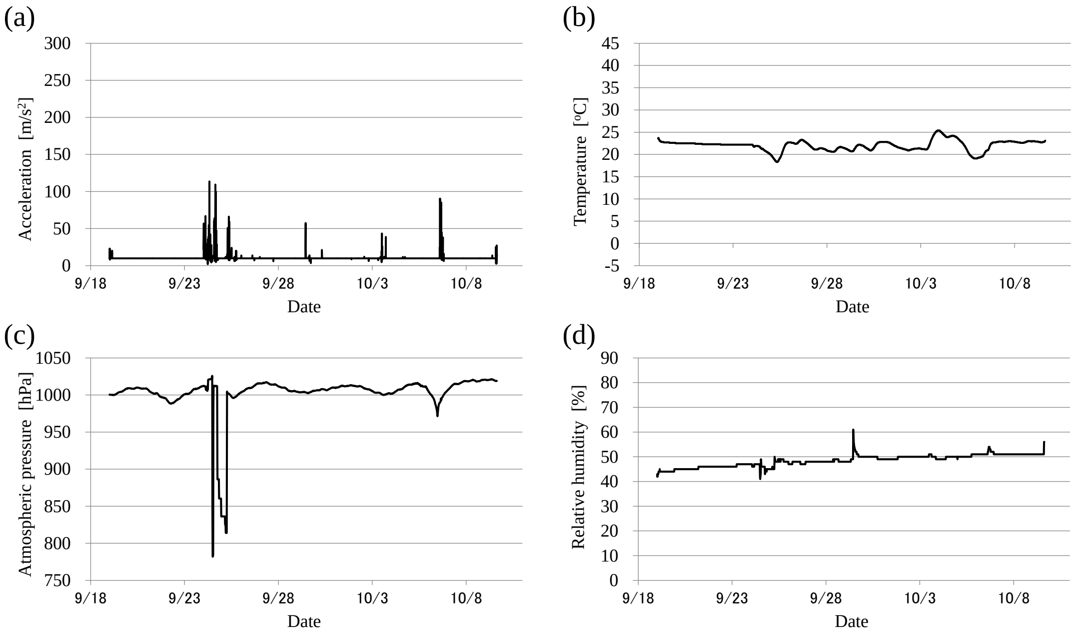

Figure 4.2: Environmental conditions during transportation from NIST to NMIJ/AIST.

5. Measurement

The general instructions for operating the pressure monitors are described in the operation manuals [7,8], which were included in the transfer package. The measurement procedure was specified in detail in the protocol [9]. Important procedures in preparations and measurements are summarized in the following subsections.

5.1 Measurement conditions and preparation

Participants prepared and used the gas medium of their usual calibrations: NMIJ/AIST used Nitrogen, while NIST used Helium. Participants also operated their pressure standards at their normal operating temperature. The effect of the gas medium and ambient temperature on the pressure monitors were evaluated by the pilot institute. The environmental conditions during measurements, i.e., atmospheric pressure, ambient temperature and relative humidity, were measured using each participant's instruments.

The transfer standard was firmly mounted on a table, and the level was adjusted using the bubble level placed on the TS base plate. The settings of the pressure monitors, such as sampling intervals, were checked according to the protocol. After the installation, TS was pressurized up to 100 MPa, and the leak in the calibration system was checked.

The pilot institute provided LabVIEW software to check the communication with the two pressure monitors and to obtain the readings of them during measurements. The participants prepared their own computer for the measurement, and established communication between the pressure monitors and the computer according to the protocol.

Pressure monitors was powered at least 24 hours before starting the measurement for warming up and stabilization.

5.2 Measurement procedures

One complete measurement cycle consists of 22 measurement points: 11 points from 0 to 100 MPa in steps of 10 MPa for ascending pressures, and 11 points from 100 to 0 MPa for descending pressures as shown in figure 5.1. The measurements of three cycles were completed with each cycle being on a separate day. No gauge pressures were applied to the pressure monitors during the 12 hours before the start of each measurement cycle.

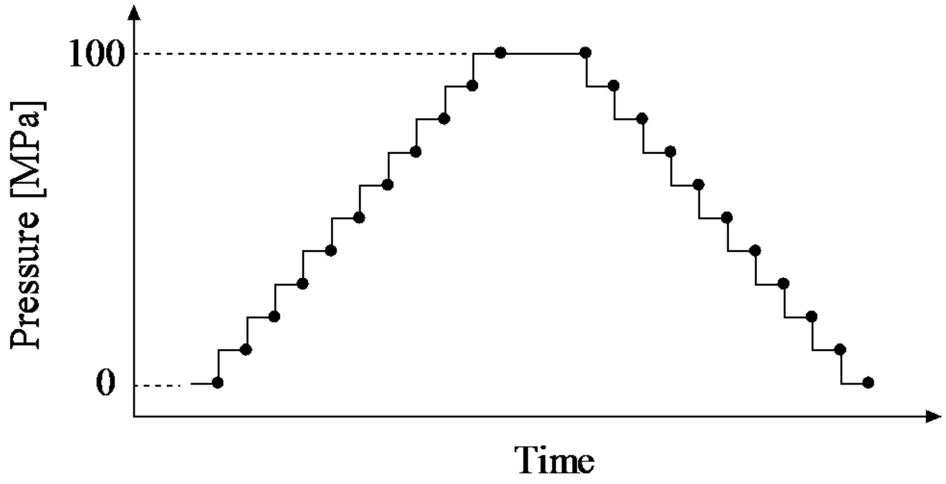

Figure 5.1: Pressure change in one measurement cycle

The time intervals in a measurement cycle, including operating time from one measurement point to the next, were also specified in the protocol, as shown in Figure 5.2. The time for changing pressure from one measurement pressure to the next was set to be within three minutes. The pressure was held constant for seven minutes for stabilization. The readings of the pressure monitors were obtained at every six seconds using the data acquisition program immediately after the waiting time. The average for the ten readings and its corresponding standard deviation were recorded as well as the raw readings of the monitors. After the first measurement at 100 MPa during the increasing part of the pressure cycle, the pressure was held at 100 MPa for 30 minutes, and then the pressure decreasing process was started with the second 100 MPa measurement.

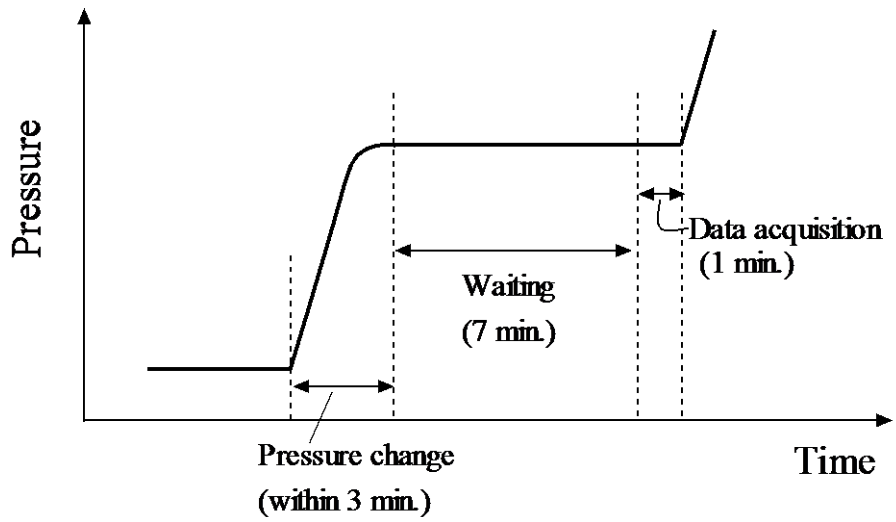

Figure 5.2: Time interval from one measurement point to the next

5.3 Reporting of the results

The participating institutes reported their results to the pilot institute using the following four kinds of sheets included in the protocol [9].

(i) Participant's standard

Information of the participant's standard used in this comparison was reported, including the type and characteristics of the piston-cylinder assembly, the effective area and its uncertainty, and the origin of its traceability to the SI. This information is summarized in section 2.1.

(ii) Measurement conditions

Details of the measurement conditions are reported. Those are local gravity, differential height of the reference levels between the participating institute's standard and the transfer standard, the kind and physical properties of the pressure medium used, power voltage and frequency applied to the pressure monitors. The instruments for measuring environmental conditions are also described. The information of the measurement conditions is listed in Table 5.1.

(iii) Results in individual cycle [1/3, 2/3, 3/3]

The measurement results at each measurement cycle were reported. The combined standard uncertainty (coverage factor $k = 1$) of the applied pressure at the reference level of the transfer standard was also included. Three sheets for the three cycles were submitted to the pilot institute.

(iv) Uncertainty budget

An uncertainty budget sheet, including a list of the principal uncertainty components, was reported on the basis of the participant's format. The standard uncertainty (coverage factor $k = 1$) was estimated and combined following the *Guide to the Expression of Uncertainty in Measurement* (GUM) [10].

5.4 Methods and parameters used by each participating institute

Details of the methods and parameters used for the measurements are listed in Table 5.1.

Table 5.1: Details of the parameters used by each participating institute. All the uncertainties are expressed as the standard ones.

		NMIJ/AIST	NIST
Local gravity			
	g [m/s^2]	9.7994804	9.801011
	$u(g)$ [m/s^2] (k=1)	5 x 10^{-7}	2 x 10^{-6}
Pressure medium			
	Gas medium	Nitrogen	Helium
	Density ρ_f [kg/ m^3]	0.1 MPa≦p≦10 MPa (-2.875x10^{-3} *p^3 + 2.598x10^{-2}* p^2 + 1.138x10*p)/ (t /296.15)) 10 MPa<p≦100 MPa (4.453x10^{-4}*p^3 – 1.207x10^{-1}*p^2 + 1.346x10*p - 9.036) / (t/296.15) p absolute pressure in MPa, t temperature in K [11]	0.162*p*9.86x10^{-6} (p absolute pressure in Pa)
	$u(\rho_f)$ [kg/ m^3] (k=1)	0.003x ρ_f	0.01x ρ_f
Height difference between the laboratory standard and the transfer standard *h* (*h* is positive when the level of the laboratory standard is higher.)			
	h [mm]	186	193
	$u(h)$ [mm] (k=1)	0.5	0.8
Power supply to the pressure monitors			
	Voltage [VAC]	100	120
	Frequency [Hz]	50	60
Instruments for measuring environmental condition			
	Room temperature	Takara thermistor instruments, Model: H211	Guildline, Model: 9540 S/N: 560182

		S/N: E605014-4	
	Uncertainty [°C] (k=1)	0.2	0.1
	Relative humidity	Takara thermistor instruments, Model: H211 S/N: E605014-4	Veriteq, Model: 2000 S/N: 04122057
	Uncertainty [%] (k=1)	3	5
	Atmospheric pressure	Druck, Model: DPI 142S S/N 120393	Paroscientific, Model: 745-16B S/N: 120393
	Uncertainty [Pa] (k=1)	2.5	0.67

6. Analysis of reported data

The main basis of this comparison is the difference between the gauge pressure applied by the participant's standard and the readings of the two pressure monitors corrected to gauge pressure, together with the measurement uncertainties. The reading of the pressure monitor at each measurement pressure p MPa is defined as,

$$\boldsymbol{R_{\mathrm{p,raw}}(i,j,k,l,m)},$$

where the meanings of the parameters (i,j,k,l,m) are as the following:

i: Participating institute,

i = 1: NMIJ/AIST, i = 2: NIST

j: Pressure monitor in the transfer standard,

j = 1: pressure monitor A (Fluke, PRM4),

j = 2: pressure monitor B (Paroscientific, Model 745)

k: Gas medium,

k = 1: Nitrogen (N_2), k = 2: Helium (He)

l: Measurement cycle,

- In case of i = 1 (NMIJ/AIST), measurement cycles in the first measurement on July 2014 are expressed by l = 1, 2, 3, and those in the second measurement on October 2014 are expressed by l = 4, 5, 6.
- In case of i = 2 (NIST), measurement cycles are denoted by l = 1, 2, 3

m: Pressurizing process,

m = 1: pressure increasing process,

m = 2: pressure decreasing process.

Similarly, the gauge pressure applied by the participant's standard is given by $p_{p,std}$ (i,k,l,m) with the same parameters. The atmospheric pressure at each measurement point, obtained by the participant's device, is given by $p_{p,atm}(i,k,l,m)$.

In this section, the following factors are addressed for the deduction and analysis of the comparison data.

- Zero pressure offsets
- Effects of temperature on the respective pressure monitors
- Calculation of the sensitivity of the respective pressure monitors
- Long-term stability of the respective pressure monitors
- Effects of gas medium on the respective pressure monitors
- Calculation of the sensitivity of the transfer standard
- Uncertainty evaluation

The participating institutes are responsible for the factors individual to their standard and measurement conditions; the data after these corrections were provided to the pilot institute. All of the correction factors explained in this section were evaluated by the pilot institute on the basis of the characterization experiments and measurement results.

6.1 Correction for zero-pressure offsets

The first step of the analysis was to correct the readings of each pressure monitor for their zero-pressure offsets. The correction was conducted for each calibration cycle. There were two 0 MPa measurement data in one cycle. The readings at the beginning of each cycle was found more stable than those at the end of the cycle, mainly because the conditions of the TS before the measurement cycle was kept similar, as specified in the protocol: "No gauge pressures are to be applied to the pressure monitors during the 12 hours before the start of each measurement cycle." Therefore, the readings at the beginning of each cycle was used for the offset correction. In addition, since the pressure monitors are absolute pressure monitors and the pressure standards operate in gauge mode, the change in atmospheric pressure was compensated. Then, the reading after the offset correction, $\boldsymbol{R_{p,C0}(i,j,k,l,m)}$, is given by:

$$\boldsymbol{R_{p,C0}(i,j,k,l,m)} \\ = [\boldsymbol{R_{p,raw}(i,j,k,l,m) - R_{0,raw}(i,j,k,l,1)}] - [\boldsymbol{p_{p,atm}(i,k,l,m) - p_{0,atm}(i,k,l,1)}],$$

where, $p_{p,atm}(i,k,l,m)$ is the atmospheric pressure at the measurement of $R_{p,raw}(i,j,k,l,m)$, while $p_{0,atm}(i,k,l,1)$ is the atmospheric pressure at the measurement of $R_{0,raw}(i,j,k,l,1)$.

6.2 Effect of temperature

When the readings of the pressure monitors are significantly affected by the temperature, the readings at each measurement point should be corrected to the value at a reference temperature.

The pressure monitor used in this comparison includes a temperature sensor so that most part of the temperature effect on the pressure-sensing element in the monitor is already compensated with the use of an internal compensation function. A residual effect of the temperature was evaluated at the pilot institute. The ambient temperature of the pressure monitor was changed from 20 ^{o}C to 26 ^{o}C, and then, temperature coefficient was calculated at each pressure point from the several calibration results. The temperature coefficient of the calibration results for the two pressure monitors is shown in Figure 6.1. The coefficient differs depending on the measurement pressure, and does not show a systematic trend with pressure, mainly due to the complexity of the internal compensation function. The values of the coefficient was at most about 3×10^{-6} /K from the figure.

The ambient temperature during the measurements was also reported by the participating institutes. Figure 6.2 shows the temperature at each participating institute, which was averaged over three cycles for each measurement point. The averaged value of the ambient temperature was 24.1 ^{o}C at NMIJ/AIST, and 23.0 ^{o}C at NIST; the difference was 1.1 K at maximum. The temperature effect was relatively small, compared with the uncertainties of the laboratory standards and repeatability (as explained in section 6.8). Then, it does not appear necessary to compensate the temperature effect. Instead, this effect was considered as an uncertainty source as explained in section 6.8.3.

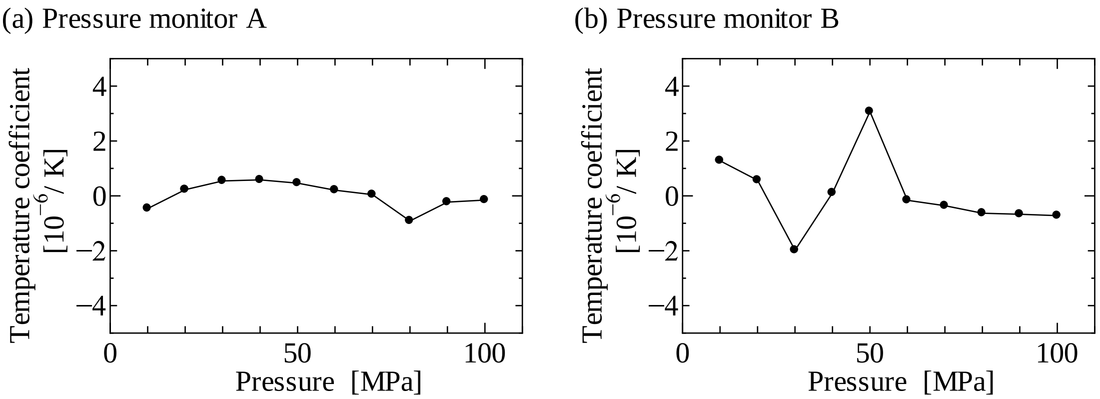

Figure 6.1: Temperature coefficient of the calibration results between 20 ^{o}C and 26 ^{o}C for the pressure monitors

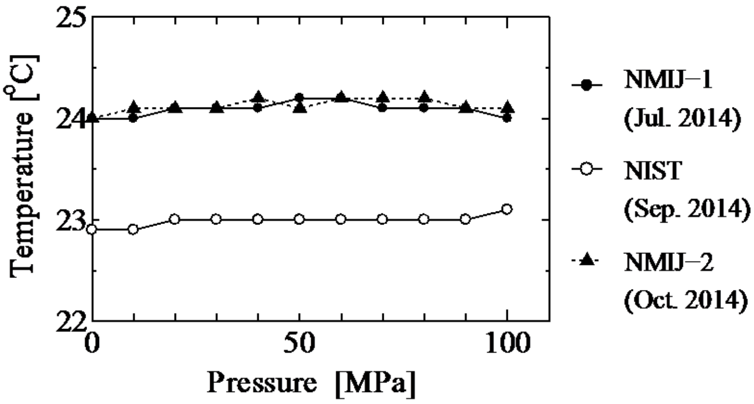

Figure 6.2: Ambient temperature during measurements at participating institutes

6.3 Calculation of sensitivity for each pressure monitor

The pressure monitors used are nominally linear devices, and so the ratio of the monitor reading to applied pressure will be essentially independent of pressure for a range of pressures around each target pressure. As the difference of actual applied pressure from the nominal pressure value was less than 0.6 % of the nominal pressure, the sensitivity at the actual applied pressure is considered equal to that at the nominal pressure. Thus, the sensitivity of each pressure monitor at each measurement point, $\boldsymbol{S}_{\mathrm{p,C0}}(\boldsymbol{i,j,k,l,m})$, is deduced as:

$$\boldsymbol{S}_{\mathrm{p,C0}}\,(\boldsymbol{i,j,k,l,m}) = \boldsymbol{R}_{\mathrm{p,C0}}\,(\boldsymbol{i,j,k,l,m})\ /\ \boldsymbol{p}_{\mathrm{p,std}}\,(\boldsymbol{i,k,l,m}).$$

There are in total six measurement data at each pressure point in a set of participant's measurements. The mean sensitivity was calculated as a simple arithmetic mean of the six data, as the following:

$$\boldsymbol{S}_{\mathrm{p,C1,NMIJ-1}}(\boldsymbol{j},\boldsymbol{k}) = \frac{\mathbf{1}}{\mathbf{6}}\sum_{l=1}^{3}\sum_{m=1}^{2}\boldsymbol{S}_{\mathrm{p,C0}}(\mathbf{1},\boldsymbol{j},\boldsymbol{k},\boldsymbol{l},\boldsymbol{m})$$

$$\boldsymbol{S}_{\mathrm{p,C1,NMIJ-2}}(\boldsymbol{j},\boldsymbol{k}) = \frac{\mathbf{1}}{\mathbf{6}}\sum_{l=4}^{6}\sum_{m=1}^{2}\boldsymbol{S}_{\mathrm{p,C0}}(\mathbf{1},\boldsymbol{j},\boldsymbol{k},\boldsymbol{l},\boldsymbol{m})$$

$$\boldsymbol{S}_{\mathrm{p,C1,NIST}}(\boldsymbol{j},\boldsymbol{k}) = \frac{\mathbf{1}}{\mathbf{6}}\sum_{l=1}^{3}\sum_{m=1}^{2}\boldsymbol{S}_{\mathrm{p,C0}}(\mathbf{2},\boldsymbol{j},\boldsymbol{k},\boldsymbol{l},\boldsymbol{m})$$

Figure 6.3 shows the deviation of the mean sensitivity from unity, $S_{\mathrm{p,C1}} - 1$, in units of 10^{-6}. Standard deviation around the mean sensitivity, $\sigma(S_{\mathrm{p,C1}})$, was also calculated and is shown in Figure 6.4, in units of 10^{-6}.

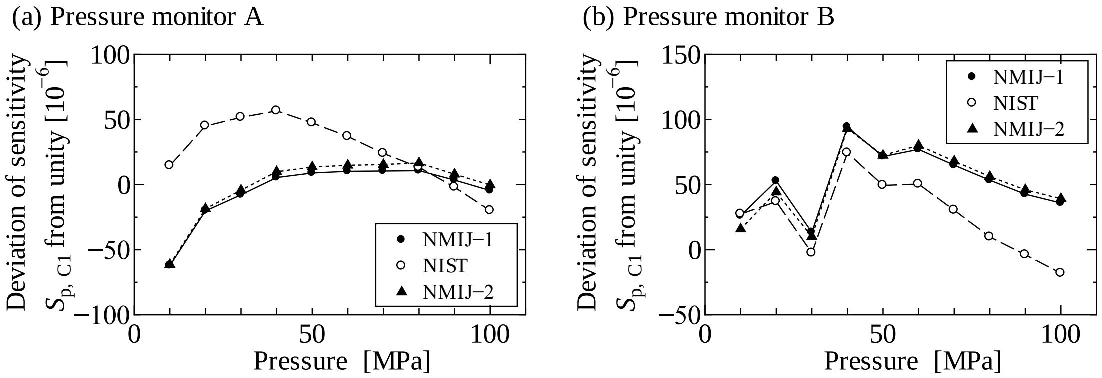

Figure 6.3: Deviation of the mean sensitivity from unity, $S_{p,C1}(i,j,k) - 1$, in units of 10^{-6}

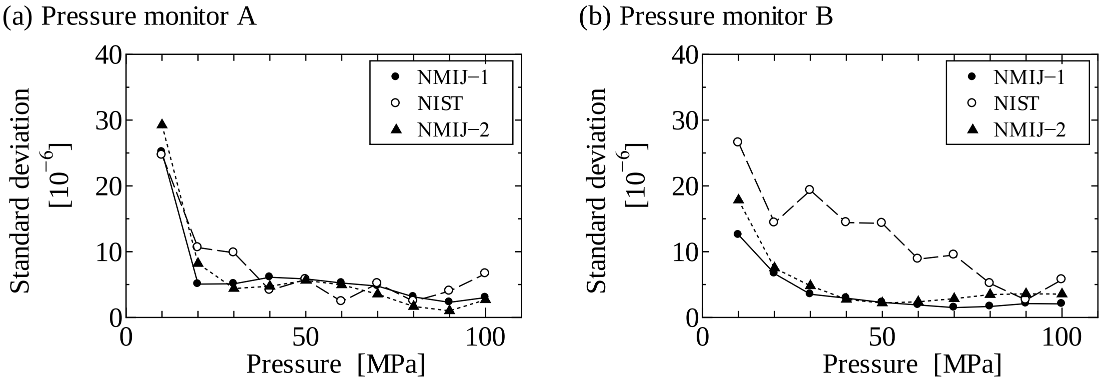

Figure 6.4: Standard deviation around the mean sensitivity $\sigma(S_{p,C1}(i,j,k))$ in units of 10^{-6}

6.4 Long-term stability

The long-term stability of the pressure monitors was evaluated from the two results at the pilot institute on July 2014 (NMIJ-1) and on October 2014 (NMIJ-2). As shown in Figure 6.3, there are no distinct difference nor shift between the two results compared with repeatability of the data. Thus, the results of the pilot institute are calculated by a simple arithmetic mean of the two mean sensitivities:

$$S_{p,C1}(1,j,k) = \frac{1}{2}\left[S_{p,C1,NMIJ\text{-}1}(j,k) + S_{p,C1,NMIJ\text{-}2}(j,k)\right]$$

$$S_{p,C1}(2,j,k) = S_{p,C1,NIST}(j,k).$$

The difference of the two results may come from the long-term instability during the measurement, then considered as an uncertainty factor of the transfer standard, as is explained in section 6.8.4.

6.5 Correction for the effect of gas medium

Participants used different gas medium for the measurement to ensure the maximum performance of their standard devices: NMIJ/AIST used Nitrogen, and NIST used Helium. Characterization experiments at the pilot institute with the two kinds of gas revealed that the calibration results of both the pressure monitors depends on the gas medium. The amount of the difference also depends on the monitors. Thus, the sensitivity of the pressure monitor was corrected to the value with Nitrogen with the use of correction term $\boldsymbol{K_{p,\,gas}(j)}$ evaluated at the pilot institute.

The correction term for each monitor was evaluated from the two sets of experiments conducted on July 2014 and October, 2014. In the experiments, the monitors were calibrated with the two kinds of gas (N_2 and He), separately. The similar stepwise procedures were used for each set of experiments, although these procedures are not completely the same as that described in the protocol in terms of waiting time and pressurizing conditions before each measurement cycle. The sensitivity was calculated for each gas medium in the same manner as explained in sections 6.1 to 6.3, and then deduced as $\boldsymbol{S'_{p,C1,N2}(j)}$ for Nitrogen, and $\boldsymbol{S'_{p,C1,He}(j)}$ for Helium. The correction term is defined as the ratio of the sensitivity with Nitrogen to Helium, as

$$K_{p,\,gas}(j) = \boldsymbol{S'_{p,C1,N2}(j) \,/\, S'_{p,C1,He}(j)}.$$

Figure 6.5 shows the correction term, $K_{p,\,gas}(j)$, for each pressure monitor. The effects of the gas medium differ depending on the monitor; $K_{p,\,gas}(1)$, for pressure monitor A, is less than unity, while $K_{p,\,gas}(2)$ is more than unity. Since the repeatability of the data was different between the measurement results on July and October, the correction term for the each monitor was calculated as a weighted mean of the two results of $K_{p,\,gas}(j)$.

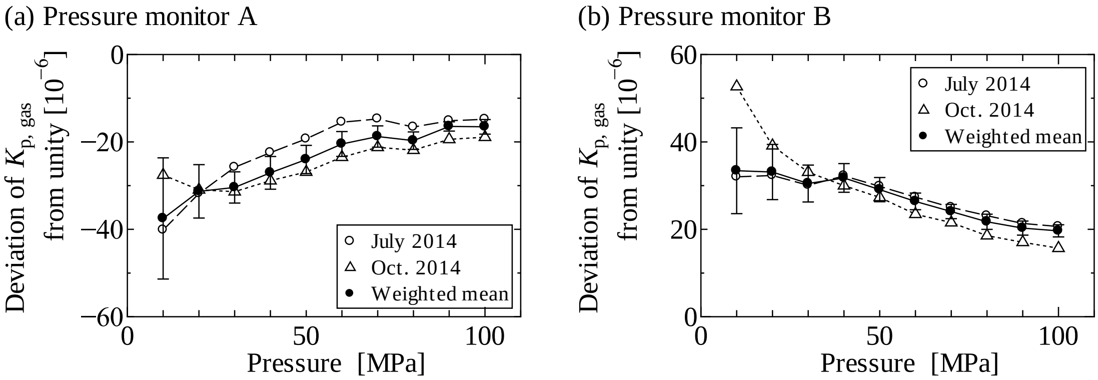

Figure 6.5: Correction term $K_{p,\,gas}$ for the effect of gas medium, in units of 10^{-6}

Finally, the sensitivity of each pressure monitor was corrected to the value with Nitrogen, $\boldsymbol{S_{p,C2}(i,j)}$, as the following:

- In case of k = 1, $S_{p,C2}(i,j) = S_{p,C1}(i,j,1)$
- In case of k = 2, $S_{p,C2}(i,j) = S_{p,C1}(i,j,2) \times K_{p,\,gas}(j)$

The corrected sensitivity $\boldsymbol{S_{p,C2}(i,j)}$ is compared between the participating institutes in Figure 6.6, in which the deviation of sensitivity from unity, $\boldsymbol{S_{p,C2}(i,j)}$– 1, is plotted against the measurement pressure.

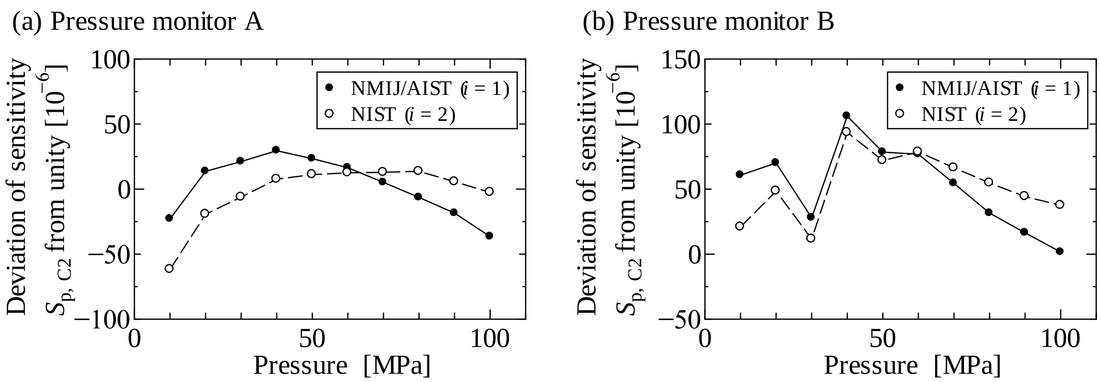

Figure 6.6: Deviation of sensitivity from unity, $\boldsymbol{S_{p,C2}(i,j)}$– 1, in units of 10^{-6}

6.6 Calculation of sensitivity of transfer standard

Figure 6.7 shows the difference of the sensitivity between NMIJ/AIST and NIST, $\boldsymbol{S_{p,C2}(2,j)}$ **-** $\boldsymbol{S_{p,C2}(1,j)}$**,** for the two pressure monitors. The two monitors showed almost the same trend in the difference, ensuring the consistency of the comparison results using the two pressure monitors.

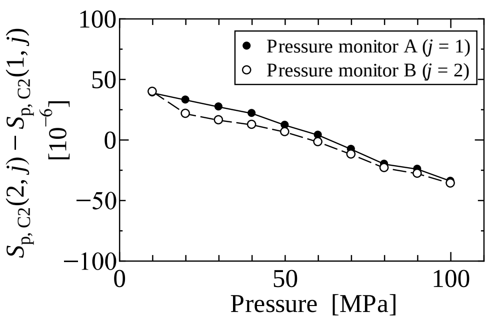

Figure 6.7: Difference of the sensitivity between NMIJ/AIST and NIST, $S_{p,C2}(2,j)$ - $S_{p,C2}(1,j)$, in units of 10^{-6}.

Finally the sensitivity of the transfer standard is calculated as a simple arithmetic mean between the two pressure monitors:

$$\boldsymbol{S}_{\mathbf{p,TS}}(\boldsymbol{i}) = \frac{\mathbf{1}}{\mathbf{2}}\sum_{\boldsymbol{j}=\mathbf{1}}^{\mathbf{2}} \boldsymbol{S}_{\mathbf{p,C2}}(\boldsymbol{i},\boldsymbol{j})$$

The results of sensitivity for the two participating institutes are compared in Figure 6.8, with error bars representing the standard (Figure 6.8(a)) and the expanded (k = 2) (Figure 6.8(b)) uncertainties, whose estimation is explained in section 6.8. In the figure, the deviation of sensitivity from unity, $\boldsymbol{S}_{\mathbf{p,TS}}$ **(*i*)**– 1, is plotted against the measurement pressure.

(a)

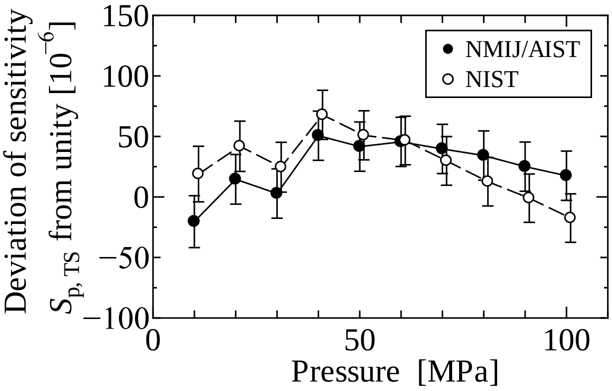

(b)

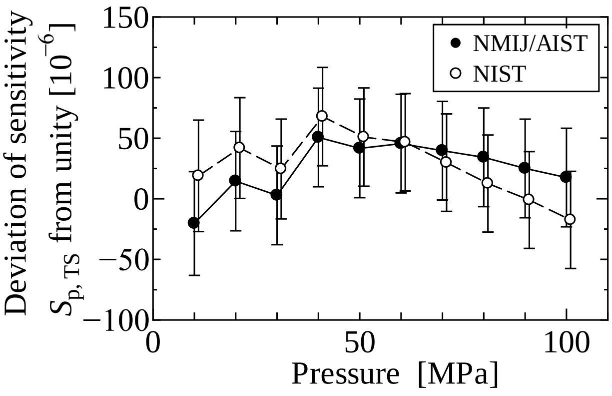

Figure 6.8: Deviation of sensitivity from unity, $\boldsymbol{S}_{\mathbf{p,TS}}$ **(*i*)**– 1, with error bars representing the standard (a) and the expanded (k = 2) (b) uncertainties.

6.7 Predicted pressure reading at nominal pressure

The predicted pressure reading for the participating institute, $R_{\mathrm{p,ex}}(i)$, is the mean reading of the transfer standard when the participating institute applies the nominal target pressure, and is calculated by

$$R_{\mathrm{p,ex}}(i) = S_{\mathrm{p,TS}}(i) \cdot P_{\mathrm{nom}}$$

where P_{nom} is the nominal value of pressure at each measurement point. The results of $R_{\mathrm{p,ex}}$ for the participating institutes are listed in Table 7.1 in section 7.1, with the comparison reference value deduced from $R_{\mathrm{p,ex}}(i)$.

6.8 Uncertainty evaluation

The combined uncertainty of the predicted pressure reading $u_{\mathrm{c}}(R_{\mathrm{p,ex}})$ for the participating institute is estimated in this subsection. From the relationship between the $S_{\mathrm{p,TS}}$ and $R_{\mathrm{p,ex}}$ explained in section 6.7, the relative uncertainty of the expected mean pressure reading is exactly the same as the uncertainty of the sensitivity. In this subsection, the combined uncertainty in the sensitivity of the transfer standard is estimated at first. Then, the uncertainty of $R_{\mathrm{p,ex}}$ is calculated as a product of the uncertainty of the sensitivity and the nominal pressure.

The combined uncertainty of the sensitivity of the transfer standard is estimated from the root-sum-square of the five uncertainty components,

$$u_{\mathrm{c}}(S_{\mathrm{p}}) = \sqrt{u_{\mathrm{std}}^2(S_{\mathrm{p}}) + u_{\mathrm{rdm}}^2(S_{\mathrm{p}}) + u_{\mathrm{tem}}^2(S_{\mathrm{p}}) + u_{\mathrm{lts}}^2(S_{\mathrm{p}}) + u_{\mathrm{gas}}^2(S_{\mathrm{p}})}$$

Each component in the right-hand side of the above equation is as the following:

$u_{\mathrm{std}}(S_{\mathrm{p}})$: Uncertainty of applied pressure from laboratory standard

$u_{\mathrm{rep}}(S_{\mathrm{p}})$: Uncertainty due to short-term random errors

$u_{\mathrm{tem}}(S_{\mathrm{p}})$: Uncertainty due to temperature effect on the transfer standard

$u_{\mathrm{lts}}(S_{\mathrm{p}})$: Uncertainty due to long-term instability of the transfer standard

$u_{\mathrm{gas}}(S_{\mathrm{p}})$: Uncertainty due to the effect of gas medium on the transfer standard

The estimations of the above uncertainty components are explained in the following subsections. Note that all the uncertainties are expressed as the standard ones in the subsections.

6.8.1 Uncertainty of applied pressure from laboratory standard

The uncertainty of the pressure applied from the participating institute's standard, $u_{\mathrm{std}}(S_{\mathrm{p}})$, is the Type B uncertainty arising from the systematic bias in the participating institute's standard. This uncertainty was reported by the participating institute for each measurement point. The main contribution of this uncertainty comes from the uncertainty of the effective area of the piston-cylinder and of its pressure distortion coefficient, It also includes the uncertainty due to the hydrostatic head correction between the reference levels of the pressure balance and the transfer standard. Table 6.1 lists the relative standard uncertainty of the applied pressure from participating institute's standard.

Table 6.1: Relative standard uncertainty of the applied pressure from participating institute's standard

i	1 (NMIJ/AIST)	2 (NIST)
Nom. Pres. [MPa]	$u_{\mathrm{std}}[S_{\mathrm{p}}(1)]$ [10^{-6}]	$u_{\mathrm{std}}[S_{\mathrm{p}}(2)]$ [10^{-6}]
10	20.0	19.6
20	20.0	19.6
30	20.0	19.6
40	20.0	19.6
50	20.0	19.6
60	20.0	19.6
70	20.0	19.6
80	20.0	19.6
90	20.0	19.6
100	20.0	19.6

6.8.2 Uncertainty due to short-term random errors

The uncertainty $u_{\mathrm{rdm}}(S_{\mathrm{p}})$ is the Type A uncertainty, and mainly comes from the combined effect of short-term random errors of the transfer standard during calibrations. The uncertainty is estimated from the standard deviation of the corrected sensitivity $\sigma(S_{\mathrm{p,C1}}(i,j))$, shown in Figure 6.4. For the pilot institute, the standard deviation of the sensitivity is calculated by the pooled variance of the standard deviations obtained in the two measurements on July and October 2014. Then, the calculation of $u_{\mathrm{rdm}}(S_{\mathrm{p}})$ for each pressure monitor and each participant is given by:

$$u^2_{\mathrm{rdm}}[S_{\mathrm{p}}(1,j)] = \frac{1}{2}\left[\frac{\sigma^2(S_{\mathrm{p,C1,NMIJ-1}})}{\sqrt{6}} + \frac{\sigma^2(S_{\mathrm{p,C1,NMIJ-2}})}{\sqrt{6}}\right]$$

$$u^2_{\mathrm{rdm}}[S_{\mathrm{p}}(2,j)] = \frac{\sigma^2(S_{\mathrm{p,C1,NIST}})}{\sqrt{6}}$$

The sensitivity of the transfer standard is a simple arithmetic mean of the sensitivities of the two pressure monitors. Then, naturally, the uncertainty due to the short-term random errors for the transfer standard $u_{\mathrm{rdm}}[S_{\mathrm{p}}(i)]$ is a root-sum-square of the half value of the standard deviation $u_{\mathrm{rdm}}[S_{\mathrm{p}}(i,j)]$, as

$$u^2_{\mathrm{rdm}}[S_{\mathrm{p}}(i)] = \frac{1}{2^2}\sum_{j=1}^{2} u^2_{\mathrm{rdm}}[S_{\mathrm{p}}(i,j)]$$

The calculated values of $u_{\mathrm{rdm}}[S_{\mathrm{p}}(i)]$ are listed in Table 6.2, and graphically shown in Figure 6.9.

Table 6.2: Uncertainty due to short-term random errors for the pressure monitors and the transfer standard

i	1 (NMIJ/AIST)			2 (NIST)		
j	1	2	(TS)	1	2	(TS)
Nom. Pres. [MPa]	$u_{rdm}[S_p(1,1)]$ [10^{-6}]	$u_{rdm}[S_p(1,2)]$ [10^{-6}]	$u_{rdm}[S_p(1)]$ [10^{-6}]	$u_{rdm}[S_p(2,1)]$ [10^{-6}]	$u_{rdm}[S_p(2,2)]$ [10^{-6}]	$u_{rdm}[S_p(2)]$ [10^{-6}]
10	11.1	6.3	6.4	10.1	10.8	7.4
20	2.8	2.9	2.0	4.3	5.9	3.6
30	1.9	1.7	1.3	4.0	7.9	4.4
40	2.2	1.2	1.3	1.7	5.9	3.1
50	2.3	0.9	1.3	2.4	5.8	3.1
60	2.1	0.9	1.1	1.0	3.6	1.9
70	1.7	0.9	1.0	2.1	3.9	2.2
80	1.0	1.1	0.8	1.0	2.1	1.2
90	0.7	1.2	0.7	1.6	1.1	1.0
100	1.2	1.2	0.8	2.7	2.3	1.8

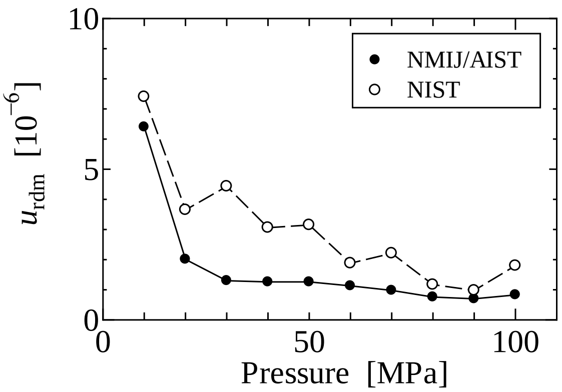

Figure 6.9: Uncertainty due to short-term random errors for the pressure standard

6.8.3 Uncertainty due to temperature effect

As explained in section 6.2, the effect of the ambient temperature on the transfer standard is considered as an uncertainty source. In Figure 6.1, the maximum value of the evaluated temperature coefficient was 3×10^{-6} /K. In Figure 6.2, the temperature difference of the two participants was 1.1 K at maximum. Then, the uncertainty due to the temperature effect on the sensitivity was roughly estimated by the product of the two values, 3.3×10^{-6} /K. The same value of the uncertainty is used for all the measurement points.

$$u_{\mathrm{tem}}[S_{\mathrm{p}}] = 3.3 \times 10^{-6}$$

6.8.4 Uncertainty due to long-term instability

As explained in section 6.4, the long-term stability of the pressure monitor was evaluated from the two measurement results at the pilot institute. Because of the limited sample of the pilot institute calibrations, a Type B evaluation was used to estimate the uncertainty for each pressure monitor. Assuming that the long-term stability is modeled by a normal distribution, the standard uncertainty equals one-half the difference between the two measurement results, as the following:

$$u_{\mathrm{lts}}[S_{\mathrm{p}}(j)] = \frac{|S_{\mathrm{p,C1,NMIJ\text{-}1}}(j) - S_{\mathrm{p,C1,NMIJ\text{-}2}}(j)|}{2}$$

Then, the standard uncertainty due to the long-term shift of the transfer standard is deduced as the following:

$$u_{\mathrm{lts}}^2[S_{\mathrm{p}}] = \frac{1}{2^2}\sum_{j=1}^{2} u_{\mathrm{lts}}^2[S_{\mathrm{p}}(i,j)]$$

The calculated values of the uncertainty are listed in Table 6.3 and shown in Figure 6.10.

Table 6.3: Standard uncertainty due to the long-term instability of the transfer standard

j	1	2	
Nom. Pres. [MPa]	$u_{\mathrm{lts}}[S_{\mathrm{p}}(1)]$ [10^{-6}]	$u_{\mathrm{lts}}[S_{\mathrm{p}}(2)]$ [10^{-6}]	$u_{\mathrm{lts}}[S_{\mathrm{p}}]$ [10^{-6}]
10	0.4	5.1	2.6
20	0.8	4.2	2.2
30	1.7	1.6	1.2
40	2.2	0.6	1.2
50	2.3	0.4	1.2
60	2.3	1.5	1.4
70	2.5	1.6	1.5
80	3.0	1.4	1.6
90	2.3	1.7	1.4
100	2.1	1.6	1.3

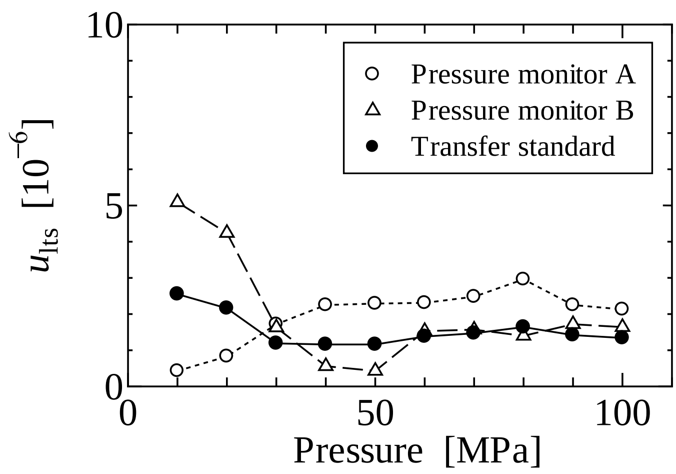

Figure 6.10: Standard uncertainty due to the long-term instability of the transfer

standard

6.8.5 Uncertainty due to the effect of gas medium

The standard uncertainty due to the effect of gas medium directly comes from the uncertainty of the correction term from He to N_2.

$$u_{\mathrm{gas}}[S_{\mathrm{p}}(j)] = u[K_{\mathrm{p,gas}}(j)]$$

The correction term of the gas medium was calculated as a weighted mean of the two experimental results on July and October 2014. The standard uncertainty for each pressure monitor was naturally calculated as a standard deviation of the weighted mean.

The standard uncertainty due to the effect of gas medium on the transfer standard is deduced from the uncertainty for the two pressure monitors, as the following:

$$u_{\mathrm{gas}}^2[S_{\mathrm{p}}] = \frac{1}{2^2}\sum_{j=1}^{2} u_{\mathrm{gas}}^2[S_{\mathrm{p}}(j)] = \frac{1}{2^2}\sum_{j=1}^{2} u^2[K_{\mathrm{p,gas}}(j)]$$

The calculated values of $u_{\mathrm{gas}}[S_{\mathrm{p}}(i)]$ are listed in Table 6.4, and shown in Figure 6.11.

Table 6.4: Standard uncertainty due to the effect of gas medium

j	1	2	
Nom. Pres. [MPa]	$u_{\mathrm{gas}}[S_{\mathrm{p}}(1)]$ [10^{-6}]	$u_{\mathrm{gas}}[S_{\mathrm{p}}(2)]$ [10^{-6}]	$u_{\mathrm{gas}}[S_{\mathrm{p}}]$ [10^{-6}]
10	13.9	9.8	8.5
20	6.1	6.3	4.4
30	3.6	4.2	2.8
40	3.7	3.3	2.5
50	3.2	2.8	2.1
60	2.8	1.9	1.7
70	2.4	1.6	1.5
80	2.0	1.7	1.3
90	1.1	1.6	1.0
100	1.7	1.4	1.1

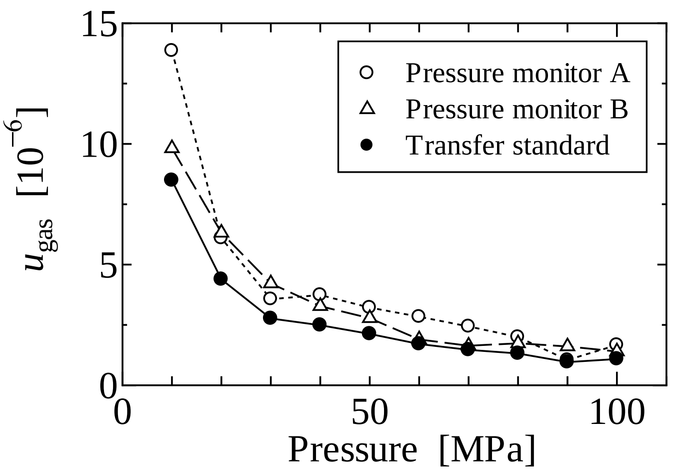

Figure 6.11: Standard uncertainty due to the effect of gas medium

6.8.6 Combined uncertainty

Combined standard uncertainty of the sensitivity is calculated from the five uncertainty components evaluated in section 6.8.1 to 6.8.5. Uncertainty budgets for the participating institutes are summarized in Table 6.5, and the combined uncertainties are plotted against measurement pressure in Figure 6.12.

Table 6.5: Uncertainty budget for the participating institutes

(a) NMIJ/AIST

Nom. Pres. [MPa]	u_{std} [10^{-6}]	u_{rdm} [10^{-6}]	u_{tem} [10^{-6}]	u_{lts} [10^{-6}]	u_{gas} [10^{-6}]	u_c [10^{-6}]	$U_c(k=2)$ [10^{-6}]
10	20.0	6.4	3.3	2.6	0.0	21.4	42.8
20	20.0	2.0	3.3	2.2	0.0	20.5	41.0
30	20.0	1.3	3.3	1.2	0.0	20.3	40.7
40	20.0	1.3	3.3	1.2	0.0	20.3	40.7
50	20.0	1.3	3.3	1.2	0.0	20.3	40.7
60	20.0	1.1	3.3	1.4	0.0	20.3	40.7
70	20.0	1.0	3.3	1.5	0.0	20.3	40.7
80	20.0	0.8	3.3	1.6	0.0	20.4	40.7
90	20.0	0.7	3.3	1.4	0.0	20.3	40.7
100	20.0	0.8	3.3	1.3	0.0	20.3	40.7

(b) NIST

Nom. Pres. [MPa]	u_{std} [10^{-6}]	u_{rdm} [10^{-6}]	u_{tem} [10^{-6}]	u_{lts} [10^{-6}]	u_{gas} [10^{-6}]	u_c [10^{-6}]	$U_c(k=2)$ [10^{-6}]
10	19.6	7.4	3.3	2.6	8.5	23.0	46.0
20	19.6	3.6	3.3	2.2	4.4	20.8	41.6
30	19.6	4.4	3.3	1.2	2.8	20.6	41.2
40	19.6	3.1	3.3	1.2	2.5	20.3	40.6
50	19.6	3.1	3.3	1.2	2.1	20.3	40.5
60	19.6	1.9	3.3	1.4	1.7	20.1	40.2
70	19.6	2.2	3.3	1.5	1.5	20.1	40.2
80	19.6	1.2	3.3	1.6	1.3	20.0	40.0
90	19.6	1.0	3.3	1.4	1.0	20.0	39.9
100	19.6	1.8	3.3	1.3	1.1	20.0	40.1

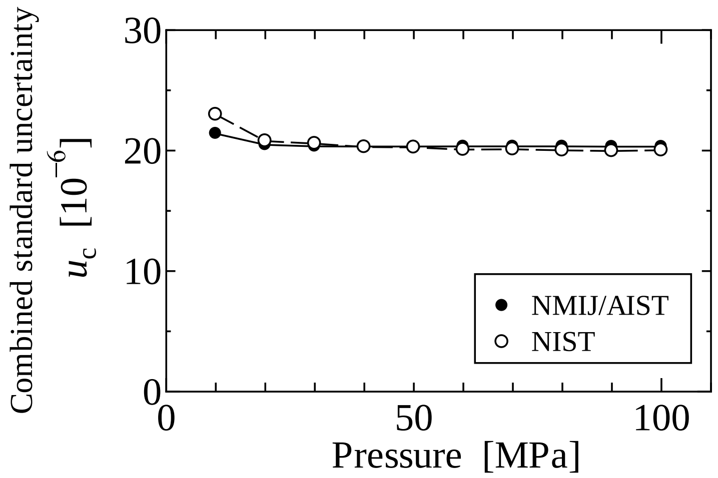

Figure 6.12: Relative combined standard uncertainty of the sensitivity of the transfer standard, in units of 10^{-6}.

Finally, the standard uncertainty of the expected mean pressure reading $u[R_{p,ex}(i)]$ is calculated by a product of the uncertainty of the sensitivity and the nominal pressure, and listed in Table 6.6.

Table 6.6: Combined standard uncertainty of the expected mean pressure reading for the participating institute

i	1 (NMIJ/AIST)	2 (NIST)
Nom. Pres. [MPa]	$u[R_{p,ex}(1)]$ [kPa]	$u[R_{p,ex}(2)]$ [kPa]
10	0.21	0.23
20	0.41	0.42
30	0.61	0.62
40	0.81	0.81
50	1.02	1.01
60	1.22	1.21
70	1.42	1.41
80	1.63	1.60
90	1.83	1.80
100	2.03	2.00

7. Results for supplementary comparison APMP.M.P-S6

7.1 Supplemental comparison reference values

Although there are several procedures to define a comparison reference value, it seems reasonable to calculate a simple arithmetic mean of the participant's results, since the combined uncertainty is almost the same for both the participating institutes. Table 7.1 lists the comparison reference value $R_{p,RV}$, calculated from the expected pressure readings of the two institutes.

Table 7.1: Expected pressure readings for the participating institutes and the comparison reference value

i	1 (NMIJ/AIST)	2 (NIST)	
Nom. Pres. [MPa]	$R_{p,ex}(1)$ [MPa]	$R_{p,ex}(2)$ [MPa]	$R_{p,RV}$ [MPa]
10	9.99980	10.00019	9.99999
20	20.00029	20.00084	20.00056
30	30.00008	30.00074	30.00041
40	40.00202	40.00271	40.00237
50	50.00208	50.00255	50.00231
60	60.00273	60.00280	60.00276
70	70.00278	70.00209	70.00243
80	80.00274	80.00101	80.00187
90	90.00225	89.99991	90.00108
100	100.00175	99.99826	100.00000

The degree of equivalence of the participating institute's result from the reference value is expressed by the two quantities: the deviation of the participating institute's result from the reference value and the expanded uncertainty of this deviation, as the following:

$$D_{p,i} = R_{p,ex}(i) - R_{p,RV}$$

$$U_{\mathrm{p},i} = ku_{\mathrm{c}}(D_{\mathrm{p},i}) = k\sqrt{\left(1-\frac{2}{N}\right)u_c^2[R_{\mathrm{p,ex}}(i)] + \frac{1}{N^2}\sum_{i}^{N} u_c^2[R_{\mathrm{p,ex}}(i)]}$$

,where N is the number of the participating institutes (N = 2), k is the coverage factor (k = 2 was used to represent the expanded uncertainty).

The two quantities, $D_{\mathrm{p},i}$ and $U_{\mathrm{p},i}$, are summarized in Table 7.2. The absolute values of $D_{\mathrm{p},i}$ /$U_{\mathrm{p},i}$ are all within the unity, meaning that the results of the participating institute are equivalent with the comparison reference values. To graphically show the relation between the values $D_{\mathrm{p},i}$ and $U_{\mathrm{p},i}$, at each measurement point, the deviation of the participating institute's result from the reference value $D_{\mathrm{p},i}$ is plotted with the error bar representing the expanded uncertainty $U_{\mathrm{p},i}$, in Figure 7.1.

Table 7.2: Degree of equivalence of the participating institute's result from the reference value

i	1 (NMIJ/AIST)			2 (NIST)		
Nom. Pres. [MPa]	D_1 [MPa]	U_1 [MPa]	D_1/U_1 [MPa]	D_2 [MPa]	U_2 [MPa]	D_2/U_2 [MPa]
10	-0.00020	0.00031	-0.63	0.00020	0.00031	0.63
20	-0.00027	0.00058	-0.47	0.00027	0.00058	0.47
30	-0.00033	0.00087	-0.38	0.00033	0.00087	0.38
40	-0.00034	0.00115	-0.30	0.00034	0.00115	0.30
50	-0.00023	0.00144	-0.16	0.00023	0.00144	0.16
60	-0.00003	0.00172	-0.02	0.00003	0.00172	0.02
70	0.00035	0.00200	0.17	-0.00035	0.00200	-0.17
80	0.00086	0.00228	0.38	-0.00086	0.00228	-0.38
90	0.00117	0.00257	0.46	-0.00117	0.00257	-0.46
100	0.00175	0.00285	0.61	-0.00175	0.00285	-0.61

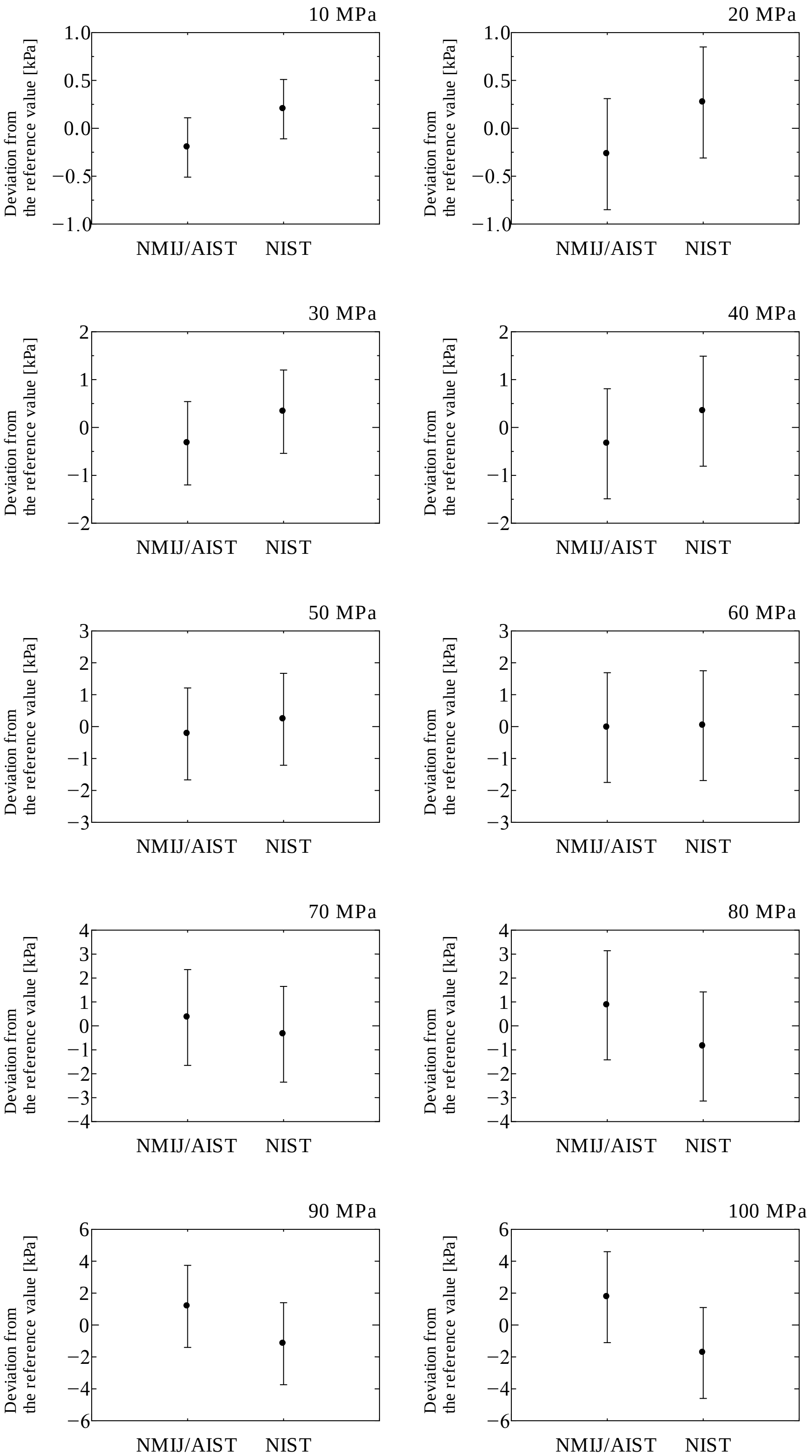

Figure 7.1: Deviation of the participating institute's results from the reference value

7.2 Degree of equivalence between the participating institutes

Degree of equivalence between the two participating institutes can be expressed at each measurement pressure by two quantities: the difference of their deviations from the reference value $D_{\mathrm{p},ii'}$ and the expanded uncertainty of this difference $U_{\mathrm{p},ii'}$. The difference of their deviations from the reference value is equal to the difference of the expected pressure readings between the two institutes, as the following:

$$D_{\mathrm{p},ii'} = (R_{\mathrm{p,ex}}(i) - R_{\mathrm{p,RV}}) - (R_{\mathrm{p,ex}}(i') - R_{\mathrm{p,RV}}) = (R_{\mathrm{p,ex}}(i) - R_{\mathrm{p,ex}}(i'))$$

The expanded uncertainty of this difference is calculated from the uncertainty of the expected mean pressure readings for the respective institutes by using the root-sum-square method,

$$U_{\mathrm{p},ii'} = ku_{\mathrm{c}}(D_{i,i'}) = k\sqrt{u_c^2[R_{\mathrm{p,ex}}(i)] + u_c^2[R_{\mathrm{p,ex}}(i')]}\ ,$$

where k is the coverage factor (k = 2 was used to represent expanded uncertainty). Since only the two institutes participated in this comparison, $D_{\mathrm{p},ii'}$ and $U_{\mathrm{p},ii'}$ are naturally rewritten by, $D_{\mathrm{p},ii'} = 2 \times D_{\mathrm{p},i}$ and $U_{\mathrm{p},ii'} = 2 \times U_{\mathrm{p},i}$. Thus, as clearly shown in Table 7.2 and Figure 7.1, the gas high-pressure standards of the two participating institutes are fully equivalent within their claimed uncertainties.

8. Discussion

The two pressure monitors used as the transfer standard were sufficiently stable. Additional information about the monitors' characteristics is provided for reference. As well as the characteristics explained in section 6, the pilot institute evaluated the effect of the attitude. The transfer standard was inclined from front to back and from side to side within 0.5 degrees with the use of bubble level mounted on the Al-plate during the measurements. The difference of the readings due to the inclination was within the data scattering measured under the same level conditions. Thus, the effect of the attitude was found negligible as long as the level of the base-plate of the TS is adjusted with the bubble level.

The pressure monitors showed shifts and slight changes in their calibration curve immediately after having been manufactured. The monitors did not show large shifts during the measurements, because the monitors had experienced a large number of pressure cycles through characterization experiments and the measurement period was relatively short. The evaluation of the long-term shift and the corrections are necessary when the measurements are carried out by many participants over a long period of time.

NMIJ/AIST is providing the high gas pressure standard with Nitrogen, while NIST is providing the standard with Helium. Then, the results with the two gas medium were compared by evaluating the correction term from the results with Helium to those with Nitrogen; this correction term of the gas medium effect was unexpectedly large for both the pressure monitors. Although the sensing mechanism is similar for both the monitors, the trend and amount of the effect depend on the individual monitors. Note that this phenomenon was reproducible, as observed both on July and October 2014, and that calibration or pressurization with one kind of gas did not affect the calibration results subsequently conducted with the other gas, as long as the gas in the tubing was completely replaced. The effect of the weight (gravitational force) of the pressure transmitting medium inside a Bourdon tube of the pressure monitor is considered to be a possible cause. Although the effect of the gas medium is appropriately corrected and also considered in the uncertainty evaluation in this comparison, identifying the cause will serve to eliminate or reduce this correction term and the corresponding uncertainty in future comparisons using different kinds of gas at high pressures.

Considering that NMIJ/AIST and NIST used different methods for their standards in terms of the kind of pressure balances, evaluation of the effective area, and the kind of gas medium, the degree of equivalence between the two standards is satisfactory to both the institutes, providing supporting evidence for CMCs of both the institutes.

9. Conclusions

A supplementary comparison of gas high-pressure standards was conducted between the National Metrology Institute of Japan (NMIJ/AIST) and the National Institute of Standards and Technology (NIST), within the framework of the Asia-Pacific Metrology Programme (APMP), in order to determine their degrees of equivalence in the pressure range from 10 MPa to 100 MPa in gauge mode. The pilot institute was NMIJ/AIST. The measurements were carried out from July 2014 to October 2014. Both the participating institutes used pressure balances as their pressure standards. The different gases were used for the pressure medium: NMIJ/AIST used Nitrogen, while NIST used Helium. A set of two pressure monitors was used as the transfer standard. The pressure monitors were found sufficiently stable during the measurements. Characteristics of the pressure monitors were evaluated at the pilot institute, and then used for data corrections and uncertainty estimations. In particular, the effect of the gas medium on the pressure monitors was found to be significant, and then all the measurement data were corrected to those with Nitrogen. The degrees of equivalence between the two institutes were evaluated by the relative differences of the participant's results and their associated combined expanded (k = 2) uncertainties. All of the results show agreements within their expanded (k = 2) uncertainties.

Acknowledgements

This comparison is supported by METI (Ministry of Economy, Trade and Industry), Japan. NMIJ/AIST participates in this comparison as part of the METI project "International Cooperation Project for Research and Standardization of Clean Energy Technologies." The invaluable advices and support by Dr. Tokihiko Kobata, the chairperson of the Technical Committee on Mass and Related Quantities (TCM) of APMP, and Dr. Kenichi Fujii, the section leader of the Pressure and Vacuum Standards Section in NMIJ, are gratefully acknowledged.

References

1. Mutual recognition of national measurement standards and of calibration and measurement certificates issued by national metrology institutes (MRA), International Committee for Weights and Measures, 1999. (http://www.bipm.org/utils/en/pdf/CIPM-MRA-2003.pdf)
2. Measurement comparisons in the CIPM MRA, CIPM MRA-D-05, version 1.5, 2014.
3. Formalities required for the CCM key comparisons (2nd revised draft), 2001.
4. Entering the details and results of RMO key and supplementary comparisons into the BIPM key comparison database, 2000.
5. Wladimir Sabuga, *et al*., "Final Report on Key Comparison CCM.P-K7 in the range 10 MPa to 100 MPa of hydraulic gauge pressure", Metrologia, Vol.42, 07005, 2005.
6. Douglas. A. Olson, "NIST calibration services for pressure using piston gauge standards", NISP SP 250-39, 2009.
7. Fluke Calibration, DH Instruments, RPM4™ Reference Pressure Monitor Operation and Maintenance Manual. (http://www.dhinstruments.com/supp1/manuals/rpm4/550129.pdf)
8. Paroscientific, Inc., Digiquartz® Pressure Instrumentation User's Manual for Model 735 Intelligent Display and Model 745 High Accuracy Laboratory Standard.

(http://www.paroscientific.com/manuals/8004-001.pdf)

9. Hiroaki Kajikawa, *et al.*, "Protocol of Asia-Pacific Metrology Program 100 MPa Gas Pressure Interlaboratory Comparison, APMP.M.P-S6", Edition 1.3, August 2014.

10. ISO/IEC 2008 Guide 98-3 Guide to the Expression of Uncertainty in Measurement (GUM: 1995), (Geneva, International Organization for Standardization), 2008.

11. J. Phys. Chem. Ref. Data, Vol. 29, No. 6, 2000